



TOGETHER
for a sustainable future

OCCASION

This publication has been made available to the public on the occasion of the 50th anniversary of the United Nations Industrial Development Organisation.



TOGETHER
for a sustainable future

DISCLAIMER

This document has been produced without formal United Nations editing. The designations employed and the presentation of the material in this document do not imply the expression of any opinion whatsoever on the part of the Secretariat of the United Nations Industrial Development Organization (UNIDO) concerning the legal status of any country, territory, city or area or of its authorities, or concerning the delimitation of its frontiers or boundaries, or its economic system or degree of development. Designations such as “developed”, “industrialized” and “developing” are intended for statistical convenience and do not necessarily express a judgment about the stage reached by a particular country or area in the development process. Mention of firm names or commercial products does not constitute an endorsement by UNIDO.

FAIR USE POLICY

Any part of this publication may be quoted and referenced for educational and research purposes without additional permission from UNIDO. However, those who make use of quoting and referencing this publication are requested to follow the Fair Use Policy of giving due credit to UNIDO.

CONTACT

Please contact publications@unido.org for further information concerning UNIDO publications.

For more information about UNIDO, please visit us at www.unido.org

Simulation of ball motion and energy transfer in a planetary ball mill*

Lu Sheng-Yong(陆胜勇)^{a)}, Mao Qiong-Jing(毛琼晶)^{a)}, Peng Zheng(彭政)^{b)},
Li Xiao-Dong(李晓东)^{a)}, and Yan Jian-Hua(严建华)^{a)†}

^{a)} State Key Laboratory of Clean Energy Utilization, Institute for Thermal Power Engineering of Zhejiang University, Hangzhou 310027, China

^{b)} Foreign Economic Cooperation Office, Ministry of Environmental Protection of People's Republic of China, Beijing 100035, China

(Received 31 October 2011; revised manuscript received 9 April 2012)

A kinetic model is proposed for simulating the trajectory of a single milling ball in a planetary ball mill, and a model is also proposed for simulating the local energy transfer during the ball milling process under no-slip condition. Based on the kinematics of ball motion, the collision frequency and power are described and the normal impact forces and effective power are derived from analyses of collision geometry. The Hertzian impact theory is applied to formulate these models, after having established some relationships among geometric, dynamic, and thermophysical parameters. Simulation is carried out based on two models, and the effects of the rotation velocity of the planetary disk Ω and the vial-to-disk speed ratio ω/Ω on other kinetic parameters have been investigated. As a result, the optimal ratio ω/Ω to obtain high impact energy in the standard operating condition at $\Omega = 800$ rpm is estimated, which is equal to 1.15.

Keywords: ball motion, energy transfer, kinetic model, milling ball

PACS: 82.20.Fd, 34.50.Ez

DOI: 10.1088/1674-1056/21/7/078201

1. Introduction

Several previous studies have reviewed the development of kinetic models related to mechanical milling. Many attempts^[1-13] have been made to simulate the kinetics of the milling process in terms of ball velocity, frequency of impact, and kinetic energy transferred to the powder during milling.^[1-13] However, the physical and chemical changes induced by the violent impact and accompanying shear forces during the milling are still puzzling. A variety of powder coalescence and fragmentation mechanisms play great roles in the milling process. The conversion efficiency of the total power, generated by an impact, to effective power transferred from the ball to the powder during an impact and the impact frequency are the two important parameters determining the efficiency of the milling process.^[1] Recent experimental researches concentrate on both the sway ball mill and the planetary ball mill: the impact velocity of the milling ball and the temperature of the vial can be experimentally

monitored during milling, and the mechanisms of energy conversion can thus be studied.

Several models for describing the kinetics and trajectory of the milling ball have been proposed by Burgio,^[5] Magini,^[6] Abdellaoui,^[9] Dallimore,^[12] and Chattopadhyay,^[13] so that both the velocity of the milling ball and its energy transfer can be calculated. Zidane *et al.*^[14] have established an equation describing the contact temperature at the impact point as a function of other parameters. A back-propagation (BP) neural network technique was applied to predict the properties of milling powders for various milling parameters and has proved suitable.^[16]

Davis *et al.*^[17] have tested the impact velocity of the milling ball in a sway SPEX mill, and obtained the results of 19 m/s (maximal) and 6 m/s (average) with the impact energy mainly ranging from 10^{-3} to 10^{-2} J. By virtue of the geometry simplified model, Maurice and Courtney^[1] predicted that the sway frequency of the SPEX mill was 1020 times per minute, and the average impact velocity was 3.9 m/s. Mu-

*Project supported by the Major State Basic Research Development Program of China (Grant No. 2011CB201500), the Science and Technology Project of Zhejiang Province, China (Grant No. 2009C13004), the National Key Technology R&D Program of China (Grant No. 2007BAC27B04-4), the Program of Introducing Talents of Disciplinary to University, China (Grant No. B08026), and Y. C. Tang Disciplinary Development Fund of Zhejiang University, China.

†Corresponding author. E-mail: yanjh@zju.edu.cn

© 2012 Chinese Physical Society and IOP Publishing Ltd

<http://iopscience.iop.org/cpb> <http://cpb.iphy.ac.cn>

las *et al.*^[18] and Loïsele *et al.*^[19] used calorimetry to test the impact speed of the SPEX mill, and obtained the results of 3.8 and 3.6 m/s, respectively. Contact temperature increases with the impact velocity in the experiment conducted by Zidane *et al.*^[14]

The operating principle in the planetary ball mill is as follows: either four or two vials are settled symmetrically on a planetary disk. Each vial rotates around its center C , as well as around the origin O located at the center of planetary disk in the opposite direction (Fig. 1); such movement confers high kinetic energy to the ball. The centrifugal force induced by rotation drives the ball to move along the vial wall, while strong friction, induced by the speed differences between the vial wall and ball, acts on the samples to be milled. As the driving speed increases, the Coriolis force (rotation bias force) forces the milling ball to leave its position from the vial wall. Subsequently, the ball starts to move inside the vial, hit the samples against the moving vial, and thus liberate massive impact momentum. The combination of impact momentum and friction force confers a high grinding capacity to the planetary ball mill.

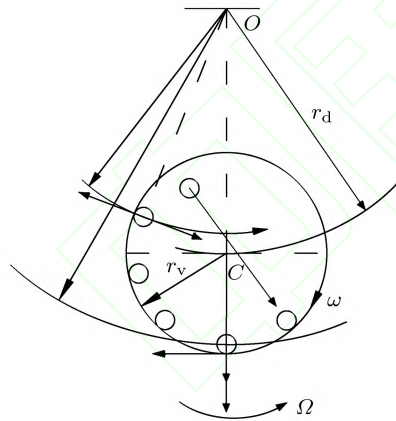


Fig. 1. Schematic drawing of the operating principle of the planetary ball mill.

2. A kinetic model for the trajectory of a single milling ball in a planetary ball mill

As shown in Fig. 2, a kinetic model is established in the Cartesian reference space on the basis of the model established by Chattopadhyay *et al.*^[13] The kinematic analysis of ball motion is presented here in

terms of a spherical Cartesian reference frame with its origin (O) located at the center of the planetary disk.^[13] Here, the distance between the origin O and center C of the vial is r_d , and r_v is the radius of the vial. The rotational speed of the disk is Ω in the anticlockwise (or normal) direction and determined by the rotational speed of the line OC . In accordance with the planetary motion of the mill, the rotational speed of the vial in the clockwise direction relative to the line OC is ω . Here, $P_0(x_0, y_0)$ is a point on the vial surface lying on the line OC , which is taken as the initial point of the ball motion.

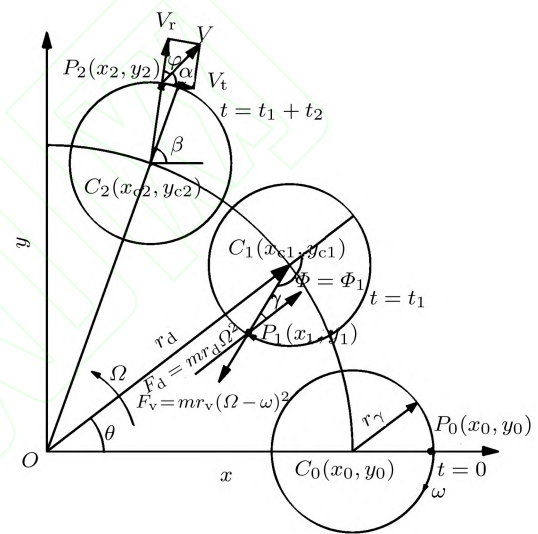


Fig. 2. Motion trajectory of a ball, showing the successive positions of the ball on the vial surface at the points of initiation ($t = 0$), detachment ($t = t_1$), and collision ($t = t_1 + t_2$).

Resolution of the centrifugal force, originating from the rotation of the vial and disk (F_v and F_d) along the direction P_1C_0 , yields the net reaction force (F_c) acting on the ball (Fig. 2). At the point of detachment (i.e., at $t = t_1$), the resultant reaction on the ball is reduced to zero (i.e., $F_c = 0$), and thus the ball leaves from the wall of the vial. The motion of the ball continues for an interval t_2 without acceleration until it collides with the vial surface (Fig. 2), thus entering the next cycle of its movement.

To simplify the analysis, the following hypotheses for the kinetic system are proposed:

- (1) The motion system in a vial, virtually involving a number of balls, is considered as the linear cumulative of a single ball motion. In other words, the balls are assumed not to interfere with each other's motion, and hence the kinematics of a single ball represents the overall process.^[5,9]

(2) The equations proposed do not take into account the slip factor, really existing during the mechanical milling process. Nevertheless they make a good approach to prove that the injected shock power is responsible for the ball milled end product.^[9] The ball adherent to the peripheral points $P_0(x_0$ and $y_0)$ or $P_2(x_2$ and $y_2)$ moves without rolling or sliding on the inner wall.

(3) After a succession of hits with the inner wall, the ball adheres to the inner wall, and then is accelerated by the vial again, ready for the next flight.

(4) The ball is regarded as a mass point.^[9]

The time period from 0 to t_1 corresponds to the interval during which the ball moves from position $P_0(x_0, y_0)$ to $P_1(x_1, y_1)$. At any instant t during this period, the position vectors \mathbf{x} and \mathbf{y} of the ball can be expressed as^[13]

$$\mathbf{x} = r_d \cos \Omega t + r_v \cos(\Omega - \omega)t, \quad (1)$$

$$\mathbf{y} = r_d \sin \Omega t + r_v \sin(\Omega - \omega)t. \quad (2)$$

Thus, the respective velocity components in the x and y directions, i.e. v_x and v_y , can be obtained

$$v_x = \frac{dx}{dt} = -\Omega r_d \sin \Omega t - (\Omega - \omega)r_v \sin(\Omega - \omega)t, \quad (3)$$

$$v_y = \frac{dy}{dt} = \Omega r_d \cos \Omega t + (\Omega - \omega)r_v \cos(\Omega - \omega)t. \quad (4)$$

The physical forces applied to the ball are its weight (gravitational action) and the vial reaction. The ball weight is negligible as compared with the vial reaction.^[9] Based on the fundamental dynamic principal, at $t = t_1$, the centrifugal force F_c acting on the ball can be obtained, which originates from the rotation of the vial and disk (F_v and F_d) and points to the axis of the vial:

$$F_c = F_v - \cos \gamma F_d, \quad (5)$$

$$F_d = m r_d \Omega^2, \quad (6)$$

$$F_v = m r_v \omega^2, \quad (7)$$

$$\gamma = \pi - \phi. \quad (8)$$

Substitute Eqs. (6)–(8) into Eq. (5), we obtain

$$F_c = m r_v \omega^2 + \cos \phi m r_d \Omega^2. \quad (9)$$

The milling ball detaches from the vial wall since $F_c \leq 0$, i.e., the take-off rotation angle ϕ_1 satisfies

$$\cos \phi_1 = -\frac{r_v(\Omega - \omega)^2}{r_d \Omega^2}. \quad (10)$$

The time required during the movement from the position $P_0(x_0, y_0)$ to $P_1(x_1, y_1)$ can be expressed as

$$t_1 = \frac{\phi_1}{\omega}. \quad (11)$$

The take-off speed (v) of the milling ball at the position $P_1(x_1, y_1)$ reads

$$v = \sqrt{\Omega^2 r_d^2 + (\Omega - \omega)^2 r_v^2 + 2\Omega(\Omega - \omega)r_v r_d \cos \phi_1}. \quad (12)$$

The position vectors for take-off and collision points $P_1(x_1, y_1)$ and $P_2(x_2, y_2)$ are relevant, i.e.,

$$\begin{aligned} & (x_2 - x_{c_2})^2 + (y_2 - y_{c_2})^2 \\ &= (x_1 - x_{c_1})^2 + (y_1 - y_{c_1})^2. \end{aligned} \quad (13)$$

The milling ball moves in a straight line, and $P_2(x_2, y_2)$ is given by

$$x_2 = x_1 + v_x t_2, \quad (14)$$

$$y_2 = y_1 + v_y t_2. \quad (15)$$

Equation (13) can be changed into a nonlinear equation with an unknown parameter t_2 , i.e.,

$$\begin{aligned} & v^2 t_2^2 + 2(x_1 v_x + y_1 v_y) t_2 \\ & - 2[x_1 r_d \cos(\phi_1 + \Omega t_2) + y_1 r_d \sin(\phi_1 + \Omega t_2)] \\ & - 2t_2 [v_x r_d \cos(\phi_1 + \Omega t_2) + v_y r_d \sin(\phi_1 + \Omega t_2)] \\ & + 2(x_1 x_{c_1} + y_1 y_{c_1}) = 0. \end{aligned} \quad (16)$$

The angle between the take-off velocity (\mathbf{v}) at the point $P_2(x_2, y_2)$ and the radial direction of the vial can be described as

$$\varphi = \beta - \alpha, \quad (17)$$

where β is the angle between the radius $C_2 P_2$ and the horizontal line, i.e., $\beta = \tan^{-1}((y_2 - y_{c_2})/(x_2 - x_{c_2}))$; α is the angle between the velocity \mathbf{v} and the horizontal line, i.e., $\alpha = \tan^{-1}(v_y/v_x)$. Substituting the above formulae into Eq. (17), we have

$$\varphi = \tan^{-1}\left(\frac{y_2 - y_{c_2}}{x_2 - x_{c_2}}\right) - \tan^{-1}\left(\frac{v_y}{v_x}\right). \quad (18)$$

A dynamic cycle of the milling ball starts from the moment when it detaches from the vial wall. After a certain time of movement t_2 , the milling ball adheres to the vial wall for a certain time t_1 . Then, the ball detaches from the vial wall and enters into the next

operation cycle. The total time for a complete cycle of ball motion can be computed according to

$$t_{\text{cycle}} = t_1 + t_2, \quad (19)$$

The frequency of ball motion is

$$f = \frac{1}{t_{\text{cycle}}}. \quad (20)$$

The impact kinetic energy of the milling ball can be calculated by

$$E_t = 0.5m_b v_r^2, \quad (21)$$

where v_r is the relative velocity of the milling ball to the vial, which can be calculated by

$$v_r = |\mathbf{v}_{\text{pi}} - \mathbf{v}_{\text{flight}}|, \quad (22)$$

where \mathbf{v}_{pi} is the velocity vector of the vial at the position $P_2(x_2, y_2)$, and $\mathbf{v}_{\text{flight}}$ is the velocity vector of the milling ball at position $P_2(x_2, y_2)$.

The impact power of the milling ball is given as follows:^[9]

$$P_t = fE_t. \quad (23)$$

3. A model for the local energy transfer during the ball milling process

In the model illustrated in Ref. [1], collision may occur over a range of impact angles, and this geometrical feature might have an important effect on the relative tendencies for coalescence and fragmentation of the powder. For example, several types of fracture can occur, depending on the impact angle, normal collision, shear friction, etc. The powder particles trapped between the colliding balls undergo severe plastic deformation, which flattens them. Under the cumulative effect of ball milling, the powder particles distributing evenly on the surface of ball become finer, leading to new surface areas.

During collision, various kinds of forces can be classified into normal collision force (F_n) and shear force (F_t), as shown in Fig. 4. The Hertzian impact theory applies, if the kinetic energy dissipation associated with the relative motion of the colliding bodies is much less than the elastic energy content of the bodies. In the model, the relative velocity of the milling balls is much less than the speed of sound in the material,

which meets the above requirement.^[18,19] We reach the following conclusions: the collisions are perfectly elastic, without energy loss; gradual compression of the milling balls is assumed, where kinetic energy is gradually transformed into stored elastic energy; since the Hertz radius (r_h) is much smaller than the radius of the milling ball, the milling surface of the collision can be assumed to be flat, as shown in Fig. 4.^[1,18]

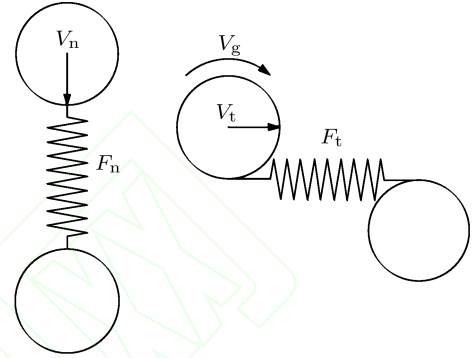


Fig. 3. (a) Normal collision force and (b) shear force acting on the milling ball during collision.

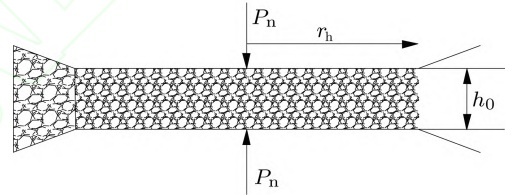


Fig. 4. The contact surface of the collision of milling balls.

The Hertzian impact theory is applied to the collisions occurring during mechanochemical treatment (MC). Thus, impact time (τ), impact radius (r_h), deformation of milling ball at maximum compression (δ_{max}), as well as normal impact pressure (P_n) and the thickness (h_0) of powder film can be calculated based on the following formulae:^[1]

$$\tau = g_\tau v_n^{-0.2} (\rho_B / E_{\text{eff}})^{0.4} r_b, \quad (24)$$

$$r_h = g_r v_n^{0.4} (\rho_B / E_{\text{eff}})^{0.2} r_b, \quad (25)$$

$$\delta_{\text{max}} = r_h^2 / 2r_b, \quad (26)$$

$$P_n = g_p v_n^{0.4} (\rho_B / E_{\text{eff}})^{0.2} E_{\text{eff}}, \quad (27)$$

$$h_0 = [16(L - 2r_b)\rho_B / 3\rho_p C_R] \times [n_B r_b^3 / (3LD_m^2 - 16n_B r_b^3)], \quad (28)$$

where g_τ , g_r , and g_p are coefficients depending on the collision geometry. Their values are given in Table 1 for some common MC configurations. The v_n is the normal impact velocity of milling balls, ρ is the density of milling balls, E_{eff} is the effective flexibility modulus of collision media, r_b is the radius of milling balls, D_m

is the diameter of the vial, L is the height inside the vial, n_B is the number of milling balls, ρ_B and ρ_p are the densities of milling balls and powder, respectively, and C_R is the ratio of milling ball mass and the power mass.

The normal impact force F_n can be given by

$$F_n = P_n \pi r_h^2. \quad (29)$$

The shear force (F_t) is a function of the tangential component (v_t) of the relative collision velocity (v_r) of milling balls and the rotation velocity (v_g), where $v_g = \omega_r r_b$, and ω_r is the rotation angular velocity. Its expression is given by

$$F_t = m \frac{d}{dt} (v_t + \omega_r r_b). \quad (30)$$

Position $P_2(x_2, y_2)$ obeys the law of conservation of momentum, i.e.,

$$\frac{d}{dt} [m v_t r_b + m (r_b^2 + r_g^2) \omega_r] = 0. \quad (31)$$

Thus, ω_r can be removed by integrating Eqs. (30) and (31)

$$F_t = - \frac{m}{(1 + r_b^2/r_g^2)} \left(\frac{dv_t}{dt} \right). \quad (32)$$

Given that the velocity of the milling ball is reduced from v_t to zero in an interval of $\tau/2$, by integrating Eq. (32) we have

$$\int_0^{\tau/2} dt = -F_t \frac{m}{(1 + r_b^2/r_g^2)} \int_{v_t}^0 dv. \quad (33)$$

Thus, the expression of shear impact force F_t can be obtained

$$F_t = \frac{m}{(1 + r_b^2/r_g^2)} \frac{2v_t}{\tau}. \quad (34)$$

The elastic energy for deformation per unit volume equals $P_n^2/2E_{\text{eff}}$, and the volume deformation caused by collision equals $2\pi r_b^2 \delta_{\text{max}}/3$. Thus, the elastic impact energy E_e and the effective power P_e per impact can be expressed as

$$E_e = \frac{\pi P_n^2 r_b^2 \delta_{\text{max}}}{6E_{\text{eff}}}, \quad (35)$$

$$P_e = f E_e. \quad (36)$$

The equation of the effective power found here will be applied to identify the optimum milling condition through mathematics, rather than experiments.

Table 1. Geometrical constants for various mill configurations. For a curved surface having a negative radius of curvature $-r_2$, χ is defined as $-r_2/r_b$.

Type of collision	g_r	g_r	g_p
Ball on ball	5.5744	0.9731	0.4646
Ball on flat surface	6.4034	1.4750	0.3521
Ball on curved surface	$6.4034[(\chi - 1)/\chi]^{0.2}$	$1.4750[\chi/(\chi - 1)]^{0.4}$	$0.3521[(\chi - 1)/\chi]^{0.6}$

4. Applications of the trajectory and energy models

4.1. Simulation of the effect of disk rotation velocity on kinetic parameters

For commercial planetary ball mills, the rotation velocity of the disk Ω and vial ω are generally in a fixed ratio. In this simulation, the variation of the ratio ω/Ω ranges from 1.0 to 2.0, covering all applications of conventional milling balls, e.g. Kexi (Nanjing), Fritsch, Retsch *et al.*, while the rotation velocity of the disk Ω ranges from 200 to 900 rpm.

The setup operating parameters and interrelated physical parameters are shown in Table 2. Figure 5 represents the variations of the frequency of collision

f , the total kinetic energy of milling ball E_t and the collision power P_t as a function of Ω ; those are obtained from Eqs. (1)–(23) established in the kinetic model for the trajectory of a single milling ball.

As shown in Fig. 5, the values of f , E_t , and P_t increase monotonically with Ω . Specifically, f increases linearly, while E_t and P_t show a parabolic increase, which is similar to that reported by Abdellaoui *et al.*^[9] and Chattopadhyay *et al.*^[13] The variation tendencies of P_t and E_t are similar to that of the ratio ω/Ω . That is to say, the values of P_t and E_t manifest a monotonic increase with the ratio ω/Ω . This is because that for a given Ω , the increase of the rotation velocity of the vial enhances the energy input to the milling ball. However, the frequency of collision f approaches its plateau and bottom at $\omega/\Omega = 1.25$ and 2,

Table 2. The operating parameters for the simulation condition.

Ω/rpm	ω/Ω	r_d/mm	r_v/mm	r_b/mm	L/mm	n_B	$\rho_B/\text{g}\cdot\text{cm}^{-3}$	m_b/g	$E_{\text{eff}}/\text{GPa}$
	1.00								
	1.25								
200–900	1.50	65	20	4.9	40	1	7.77	3.6	210
	1.75								
	2.00								

respectively, for a given level of Ω . Since the variations of the angle of incidence and the distance of movement resulted from the ratio ω/Ω leads to the variation of f .

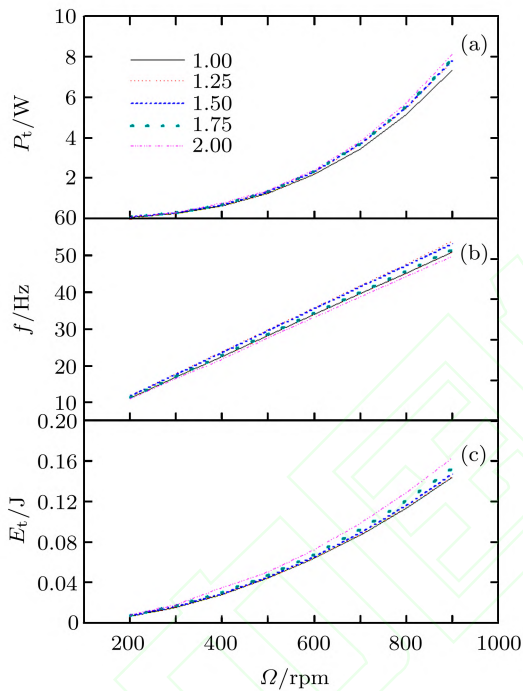


Fig. 5. (colour online) Variations of (a) the collision power P_t , (b) the collision frequency f , (c) the total kinetic energy E_t as functions of the rotation velocity of the planetary disk Ω for different levels of the vial-to-disk speed ratio ω/Ω .

The present simulation has confirmed^[13] that the level of f is determined by both ω and Ω , but the limiting value of f is determined by the ratio ω/Ω . There is a difference in the variation of P_t with ω between the report of Chattopadhyay *et al.*^[13] and the present simulation result: P_t depends on ω evidently rather than E_t in the former research; while in the latter one, both P_t and E_t manifest a small increase with ω , which may be due to that the ratio $\omega/\Omega > 1$.

Figure 6 represents the variations of the normal impact force F_n , the shearing force F_t , and the normal pressure P_n as functions of Ω , which are obtained from Eqs. (24)–(36) established in the model for the local

energy transfer during the ball milling process and the defined collision relative velocity v_r and angular φ .

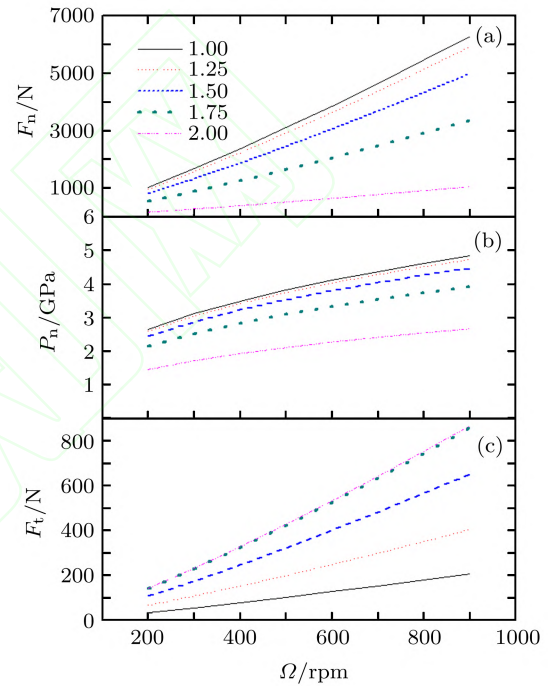


Fig. 6. (colour online) Variations of (a) the normal impact force F_n , (b) the normal pressure P_n , and (c) the shearing force F_t as functions of the rotation velocity of the planetary disk Ω for different levels of the vial-to-disk speed ratio ω/Ω .

As shown in Fig. 6, F_n , F_t , and P_n manifest a monotonic increase with Ω . The values of F_n and P_n gradually decrease while F_t increases with the increase of ratio ω/Ω for a given level of Ω , since the collision angular φ exhibits a gradual increase with the ratio ω/Ω . The results obtained are in good agreement with that obtained by Chattopadhyay *et al.*^[13]

4.2. Simulation of the influence of ratio ω/Ω on kinetic parameters

It has been proved that the milling ball becomes adherent to the vial wall, without rolling or sliding on the inner wall, when the value of ω/Ω is either less than 0.7 or greater than 3.17. Consequently, we focus

on the variation of ω/Ω in a range from 0.7 to 3.17. In addition, the rotation velocity of the disk ranges from 200 to 900 rpm, and the values of other relevant parameter are summarized in Table 3.

As shown in Fig. 7, the velocity of collision v_r manifests a gradual increase with both Ω and ω/Ω , which is consistent with the variations of E_t and P_t , as reported in Section 3.1. As the ratio ω/Ω increases, the angle between impact direction and vial wall gradually declines from 90° to 0° at $\omega/\Omega = 2.17$, increases gradually until becoming perpendicular to the vial wall, then declines again until tangentially adherent to the vial wall. When $\omega/\Omega > 3.179$, the milling ball no longer detaches from the vial wall to move into the vial, since the centrifugal force originating from the rotation of the vial is much greater than that of the disk. Thus, the angle of collision depends primarily on ω/Ω . The kinetic trajectory of a milling ball is defined for a given ratio ω/Ω ; while the collision velocity is determined by Ω and ω/Ω .

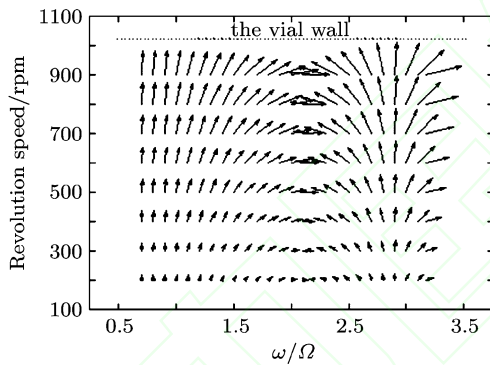


Fig. 7. Vector relationships between the velocity of collision (v_r) of the milling ball and the rotation velocity of the disk Ω and the vial-to-disk speed ratio ω/Ω .

According to the results reported previously, the variations of certain kinetic parameters including f , E_t , P_t , F_n , F_t , and P_n with Ω are similar. Thus, the variations of these parameters with ω/Ω can be studied for a given Ω .

As shown in Fig. 8, the simulation calculation is carried out at $\Omega = 800$ rpm. The values of v_r and P_t increase monotonically with ω/Ω . Since the rotation velocity of the vial increases gradually with ω/Ω ,

the v_r and P_t increase with the kinetic energy of the system input. While the increasing tendencies of v_r and P_t are different since the frequency of collision increases non-monotonically.

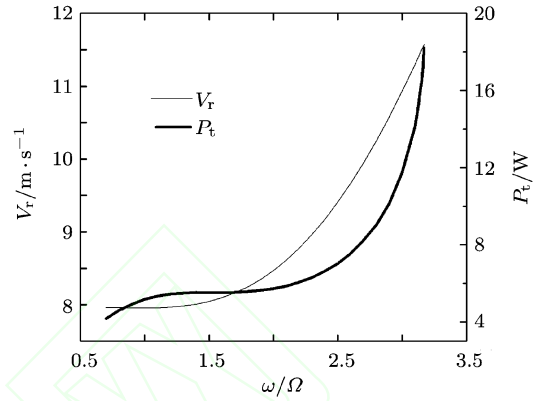


Fig. 8. Relationships between the velocity of collision v_r , the collision frequency f , the collision power P_t , and the vial-to-disk speed ratio ω/Ω at $\Omega = 800$ rpm.

As shown in Fig. 9, the frequency of collision frequency f increases to a peak at $\omega/\Omega = 1.4$, then decreases to its minimal value at $\omega/\Omega = 2.3$, and finally approaches its maximum rapidly. The value of f is determined by the operating cycle $t_{\text{cycle}} = t_1 + t_2$. As the ratio ω/Ω increases, t_1 decreases, and t_2 increases to its maximum at $\omega/\Omega = 2.3$, and then decreases to 0, i.e., the ball becomes adherent to the vial wall.

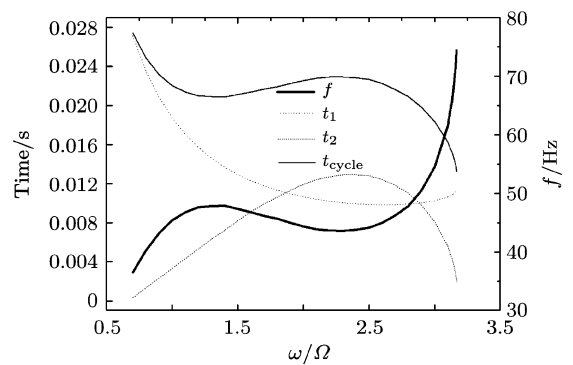


Fig. 9. Relationships between solid time t_1 , moving time t_2 , the operating cycle t_{cycle} , the collision frequency f , and the vial-to-disk speed ratio ω/Ω at $\Omega = 800$ rpm.

Table 3. The values of operating parameter.

Ω /rpm	ω/Ω	r_d /mm	r_v /mm	r_b /mm	L /mm	n_B	ρ_B /g · cm ⁻³	m_b /g	E_{eff} /GPa
200–900	0.7–3.17	65	20	4.9	40	1	7.77	3.6	210

As shown in Fig. 10, the normal impact force F_n decreases gradually to 0 with the increase of ω/Ω at $\omega/\Omega = 2.17$, and then increases monotonically to its maximum at $\omega/\Omega = 2.86$, and finally decreases to 0. The shear force F_t increases to a peak at $\omega/\Omega = 1.90$, decreases slightly until $\omega/\Omega = 2.10$, increases to another peak at $\omega/\Omega = 2.40$, decreases to 0 at $\omega/\Omega = 2.86$, and increases afterwards.

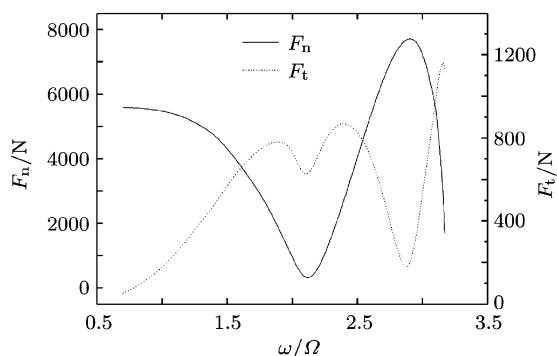


Fig. 10. Relationships between normal impact force F_n , shear force F_t , and the vial-to-disk speed ratio ω/Ω at $\Omega = 800$ rpm.

The effective power P_e per impact is an important parameter to measure the kinetic energy transferred by the ball, which greatly affect the powder by collision, leading to the mechanochemical reaction. The conversion efficiency η_t reflects the conversion efficiency from total power to effective power: $\eta_t = P_e/P_t \times 100\%$. As shown in Fig. 11, P_e increases smoothly with ω/Ω at first, and reaches its first peak at $\omega/\Omega = 1.15$. Then, it decreases to its minimal value at $\omega/\Omega = 2.17$ and increases to another peak at $\omega/\Omega = 2.86$. Finally, it decreases rapidly. Despite the monotonic increase of the total power with ω/Ω , there are two peaks of the conversion efficiency η_t which exit close to the two peaks of P_e , respectively.

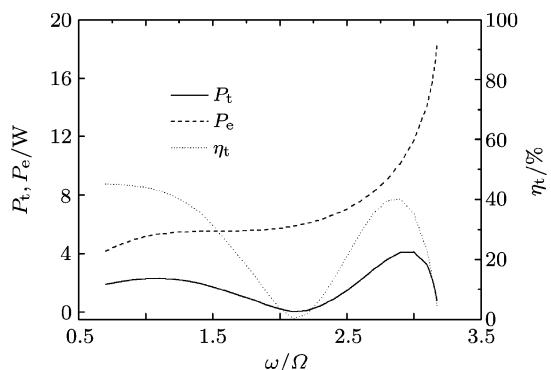


Fig. 11. Relationships between the total kinetic energy P_t , the effective power P_e , the conversion efficiency η_t , and the vial-to-disk speed ratio ω/Ω at $\Omega = 800$ rpm.

From the theoretical viewpoint, the optimal operating condition should be chosen at $\omega/\Omega=1.15$ or 2.86 in order to obtain the highest impact energy. However, since the rotation velocities of the disk and vial are generally in a fixed ratio for commercially-applied planetary ball mills, the ratio ω/Ω is required to be below 2. Conventional ball mills, e.g. Fritsch P5 and Retsch P7, have $\omega/\Omega = 1.25$ and $\omega/\Omega = 1$, respectively, thus to obtain high impact energy.

5. Conclusions

The trajectory and energy models presented here illustrate the relationships between the kinetic and dynamic parameters. The effects of the rotation velocity of the disk Ω and the vial-to-disk speed ratio ω/Ω on other kinetic parameters have been studied. All other kinetic parameters increase monotonously with the increase of the rotation velocity Ω . With the variation of the ratio ω/Ω , the impact angle of the milling ball ϕ ranges from 90° to 0° . Thus, the ideal values of the normal impact force F_n and tangential force F_t can be obtained. When the dynamic parameters of the planetary ball mill are given, the highest impact energy P_e can be obtained for the optimal value of ω/Ω . The optimal ratio ω/Ω is found to be 1.15 at $\Omega = 800$ rpm.

The established models can improved by taking account of the slip factor. Nevertheless, this work verifies the practical consistency of the models, and provides a governing principle to predict an optimal milling condition. The application of the models can predict the parameters needed to obtain a certain and optimal milling condition with higher milling efficiency.

References

- [1] Maurice D R and Courtney T H 1990 *Metall. Mater. Trans. A* **21** 289
- [2] Maurice D R and Courtney T H 1994 *Metall. Mater. Trans. A* **25** 147
- [3] Maurice D R and Courtney T H 1996 *Scripta Mater.* **34** 5
- [4] Courtney T H 1995 *Mater. Trans.* **36** 110
- [5] Burgio N, Iasonna A, Magini M, Martelli S and Padella F 1991 *Nuova Cimento Della Societa Italiana Di Fisica D* **13** 459
- [6] Magini M and Iasonna A 1995 *Mater. Trans.* **36** 123
- [7] Iasonna A and Magini M 1996 *Acta Mater.* **44** 1109
- [8] Magini M, Colella C, Iasonna A and Padella F 1998 *Acta Mater.* **46** 2841

- [9] Abdellaoui M and Gaffet E 1995 *Acta Metall. et Mater.* **43** 1087
- [10] Gaffet E 1991 *Mater. Sci. Eng. A* **132** 181
- [11] Gaffet E, Abdellaoui M and Malhouroux-Gaffet N 1995 *Mater. Trans.* **36** 198
- [12] Dallimore M P and McCormick P G 1996 *Mater. Trans.* **37** 1091
- [13] Chattopadhyay P P, Manna I, Talapatra S and Kabi S K 2001 *Mater. Chem. Phys.* **68** 85
- [14] Zidane D, Bergheul S, Rezoug T and Hadji M 2011 *J. Mater. Eng. Perform.* **20** 1109
- [15] Tafat A, Haddad A, Bergheul S and Azzaz M 2008 *Int. J. Microstruct. Mater. Prop.* **3** 791
- [16] Ma J, Zhu S G, Wu C X and Zhang M L 2009 *Mater. Des.* **30** 2867
- [17] Davis R M, McDermott B T and Koch C C 1988 *Metall. Trans.* **19** 2867
- [18] Mulas G, Deloqui F, Monagheddu M, Schiffini L and Cocco G 1997 *Mater. Sci. Forum.* **269** 693
- [19] Loiselle S, Branca M, Mulas G and Cocco G 1997 *Environ. Sci. Technol.* **31** 261
- [20] Gilman P S and Benjamin J S 1983 *Annu. Rev. Mater. Sci.* **13** 279
- [21] Zhang H, Liu G L and Qi K Z 2010 *Chin. Phys. B* **19** 048601

